

## Lateral translation of an Xe atom on metal surfaces

To cite this article: A Buldum *et al* 1995 *J. Phys.: Condens. Matter* **7** 8487

View the [article online](#) for updates and enhancements.

### Related content

- [Theoretical modelling of STM, STS and AFM](#)  
D Drakova
- [Scanning tunnelling microscopy studies of metal surfaces](#)  
Flemming Besenbacher
- [Modelling the manipulation of C60 on the Si\(001\) surface performed with NC-AFM](#)  
N Martsinovich and L Kantorovich

### Recent citations

- [Theoretical study of boundary lubrication](#)  
A. Buldum and S. Ciraci
- [Atomic Scale Sliding and Rolling of Carbon Nanotubes](#)  
A. Buldum and Jian Ping Lu
- [van der Waals atomic trap in a scanning-tunneling-microscope junction: Tip shape, dynamical effects, and tunnel current signatures](#)  
X. Bouju and Ch. Girard



**IOP | ebooks™**

Bringing you innovative digital publishing with leading voices to create your essential collection of books in STEM research.

Start exploring the collection - download the first chapter of every title for free.

# Lateral translation of an Xe atom on metal surfaces

A Buldum†, S Ciraci† and Ş Erkoç‡

† Department of Physics, Bilkent University, 06533 Ankara, Turkey

‡ Department of Physics, Middle East Technical University, 06531 Ankara, Turkey

Received 20 December 1994

**Abstract.** This work presents the theoretical study of the controlled lateral translation of an Xe atom physisorbed on the Ni(110) surface. The motion of the Xe is manipulated by the tip of the scanning tunnelling microscope. The interaction of the physisorbed atom with the tip and sample surface is described by empirical potentials. Using molecular statics and dynamics, the energetics and different modes of the translation are revealed. Important effects of electrode relaxation, tip geometry and material parameters are briefly discussed.

## 1. Introduction

Eigler and Schweizer [1] demonstrated that, using a scanning tunnelling microscope (STM), the Xe atoms physisorbed on the Ni(110) surface can be relocated at desired positions with atomic precision. Atomic relocation involved the following sequence. First the physisorbed atom is located on the Ni surface by operating the STM in the conventional tunnelling regime. Subsequently, by lowering the tip and hence increasing the interaction between the tip and adatom, the Xe atom is dragged behind the tip. Once the desired position on the substrate surface is reached the Xe atom is left behind by lifting the tip.

During the last two decades tremendous efforts on the subject of chemisorption and physisorption have been mainly concerned with the statics of the adatoms on various solid surfaces. In this respect, the work by Eigler and Schweizer opened a field with a wide range of interest covering the controlled dynamics of atoms and modification of entities (such as solid surfaces, clusters and molecules) on the atomic scale. Our knowledge in this new field is, however, rather limited. Several issues, such as the role of tip-induced local deformations together with the effect of structural and material parameters of electrodes, are crucial and require further investigation. Not only attractive or repulsive interaction between the adatom and the electrodes, but also local excitations induced by a tunnelling electron or photon may be involved in the dynamics of the adsorbed atom [2,3]. In some cases the local electric field constructed through the dipole between adatom and substrate may be efficient to lower the energy barrier in the controlled motion [3].

The character of the interaction between the adatom and the electrodes determines the nature of the bond and adsorption site. The binding energy of open-shell atoms on the metal electrode is strong owing to the significant charge (transfer and) rearrangements. Therefore, atomic scale modification of surfaces and dynamics of chemisorbed atoms may involve significant barriers to overcome, whereas closed-shell atoms engage in weak interaction with a metal surface resulting in weak physisorption bonds.

In this work we investigate the motion of an Xe atom on the Ni(110) surface manipulated by a W tip of the STM. Our objective is to develop an understanding for the controlled

motion of observed atoms and local atomic modifications rather than to perform computer simulations of the experiment. To this end we carried out potential energy surface, molecular statics and dynamics calculations on rigid, as well as relaxed electrodes by using empirical potentials. We analysed the forces and the path of the Xe in the course of controlled motion as a function of tip-sample separation.

## 2. Interaction potential and atomic model

The binding between an open-shell adatom and metal surface leading to the (ionic or covalent) bond is rather strong owing to the significant charge rearrangement. The chemisorption energy is in the range of 1–2 eV. In contrast, marginal charge rearrangement occurs in the bond formed between a closed-shell atom (such as Ar or Xe) and a metal surface. Consequently, the resulting chemical interaction becomes weak. In the Eigler–Schweizer [1] experiment the translation of Xe took place under the weak attractive force exerted by the tip. The interaction energy (and force) between the adatom and metal surface has three components at very low temperature. These are (i) chemical interaction due to the charge rearrangement (or charge transfer) which increases the binding energy; (ii) the repulsive Coulombic interaction which decreases the binding energy; (iii) the weak Van der Waals interaction which contributes to the binding energy [4]. The repulsive interaction becomes significant only for surface–adatom distances smaller than the equilibrium distance  $a_0$ . Earlier it was argued that the binding between a closed-shell adatom and metal surface is dominated by the Van der Waals interaction [5]. This interaction energy is described by an asymptotic interaction law,  $-C_n r_{ia}^{-n}$ ,  $r_{ia}$  being the distance between the metal atom and adatom [5, 6]. The contribution of the short-range chemical interaction to the binding is usually omitted. In contrast to that assertion, the self-consistent field pseudopotential calculation of Xe adsorbed on the Al(100) surface resulted in the binding energy of  $\sim 130$  meV at the hollow site [7, 8]. This binding energy includes repulsive as well as chemical interaction together with the exchange–correlation energy obtained in the local density approximation (LDA). Since the experimental binding energy is approximately 200 meV [9], the LDA binding energy has to be comparable to the Van der Waals energy. The important conclusion one draws from this result is that the charge rearrangement (or charge transfer) between a closed-shell adatom and metal surface is small but must be taken into account in many physical phenomena. The effective charge on the 6s resonance of Xe on the Pt(111) surface and charge transfer from Xe to the surface have been extensively discussed in recent works [10].

In order to investigate the overall behaviour of the controlled lateral motion we represent the interaction between the Xe atom and metal surface by an empirical potential and carry out molecular statics and dynamics calculations. This interaction potential (energy) of a single Xe atom ( $a$ ) at  $r$  with one of the electrodes ( $i = t$ , tip, and  $i = s$ , sample surface) is site dependent for small separation, but becomes uncorrugated at large distance. By expressing the interaction between an electrode atom and Xe in terms of a pair potential of Lennard-Jones type

$$U_{ia}(|r - R_i|) = \epsilon \left[ \left\{ \frac{|r - R_i|}{r_0} \right\}^{12} - 2 \left\{ \frac{|r - R_i|}{r_0} \right\}^6 \right] \quad (1)$$

one can obtain an expression for the interaction potential which determines the motion of the Xe atom. That is

$$U(r, \dots, R_i, \dots, T_m) = C \sum_l U_{sa}(|r - R_l|) + C \sum_m U_{ta}(|r - T_m|)$$

$$\begin{aligned}
 &+C_b \sum_{l>m} U_{ss}(|\mathbf{R}_l - \mathbf{R}_m|) + C_b \sum_{n>m} U_{tt}(|\mathbf{T}_n - \mathbf{T}_m|) \\
 &+C_b \sum_{l>n} U_{st}(|\mathbf{R}_l - \mathbf{T}_n|).
 \end{aligned}
 \tag{2}$$

Here,  $\mathbf{R}_l$  and  $\mathbf{T}_m$  are the position vectors of atoms of the substrate and tip, respectively. The constants  $C$  and  $C_b$  are the scaling factors which take into account the many-body effects for surface and bulk potentials, respectively. The parameters  $\epsilon$  and  $r_0$  for  $i$ - $i$  interactions are determined by using the pair potential parameters [11, 12] of the corresponding diatomic molecules and bulk stability conditions. Since the heat of adsorption of Xe atom and its height on various surfaces of Ni and W crystals are available,  $\epsilon$  and  $r_0$  of  $U_{ia}$  are determined by fitting the calculated heat of adsorption and the optimum height of Xe on the corresponding surface [13, 14].

Owing to their closed-shell electronic structure the interactions between Xe atoms have been conveniently described by the two-body Lennard-Jones-type potential. As for the interaction between Xe and a metal surface, additional terms beyond the central force term may be required. Moreover, the short-ranged (chemical) interaction can be better presented by additional exponential terms. Since not many experimental data are available for Xe-W and Xe-Ni(110) systems to fit parameters of these additional terms, we have to be content with the empirical potential given in equation (2). A potential of similar type has been used by Cerda *et al* [15]. The parameters obtained for the Xe adatom interacting with the Ni(110) metal surface and the W(111) tip are given in table 1. In the calculations with the rigid tip and sample (in which the position vectors of the electrode atoms  $\mathbf{R}_l$  and  $\mathbf{T}_m$  are fixed in their bulk positions) the terms  $U_{ss}$  and  $U_{tt}$  and  $U_{st}$  in equation (2) are omitted. Our results reported in this paper correspond to a substrate which is represented by 12 716 Ni atoms in 34 layers each containing 374 atoms. The tip is constructed by 2027 W atoms in a pyramidal geometry generated from the W(111) planes containing 22 layers. In figure 1 the schematic description of the Ni(110) surface and W(111) tip is presented. The coordinates of Xe and the apex of the tip relative to an origin on the substrate surface are denoted by  $(\xi, \kappa, \zeta)$  and  $(x, y, z)$ , respectively.

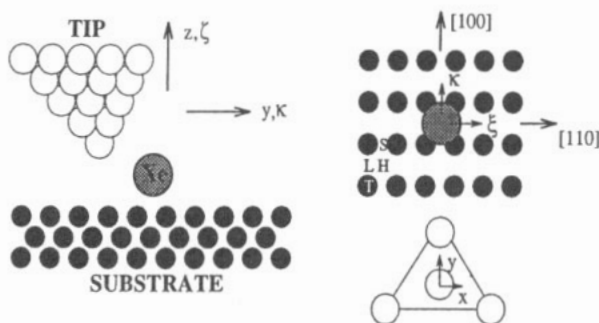


**Figure 1.** (a) Schematic description of the W(111) tip manipulating the motion of the Xe atom adsorbed on the Ni(110) surface. (b) The top view of the Ni(110) surface with the Xe atom adsorbed at the hollow (H) site.  $(x, y, z)$  and  $(\xi, \kappa, \zeta)$  are the coordinates of the tip and Xe relative to an origin on the substrate surface, respectively. The hollow (H), top (T), short-bridge (S) and long-bridge (L) sites are also shown.

**Table 1.** Values of various parameters used in equations (1) and (2).

Interaction	$\epsilon$ (eV)	$r_0$ (Å)	$C_b$	$C$
Xe-Ni	0.218	3.27		0.15658
Xe-W	0.339	3.62		0.14829
Ni-Ni	2.07	2.56	0.128034	
W-W	5.00	2.82	0.112344	
Ni-W	0.38584	2.69	1.000000	

**Table 2.** Binding energies  $E_b$  and barrier energies  $Q$  calculated for the Xe atom adsorbed on the Ni(110) surface.

Binding energy $E_b$ (meV)	Barrier energy $Q$ (meV)
H site	280
T site	151
L site	234
S site	178

### 3. Potential energy surfaces

The adsorption site and the energy barriers related to the translation of Xe on the Ni(110) surface can conveniently be analysed by calculating the potential energy surfaces. For a rigid electrode,  $U(r)$  is minimized by varying the height of the Xe atom  $\zeta$  at each grid point  $(\xi, \kappa)$  on the substrate surface. Figure 2 shows three potential energy surface which are relevant for our study. Figures 2(a) and (b) are the energy surfaces corresponding to Xe on the flat Ni(110) surface and Xe on the pyramidal W(111) tip. Figure 2(c) shows the potential energy surface of Xe on the Ni(110) surface in the presence of the W(111) tip at a given height from the surface. In agreement with previous calculation [15] the Xe atom is physisorbed at the hollow (H) site with the binding energy  $E_b = 280$  meV. The energy barrier  $Q_L$  across the long-bridge site (L) is lower than that,  $Q_S$ , across the short-bridge site(s). The energetics obtained by the two-body potential are outlined in table 2. For the W(111) tip, the Xe atom has the lowest binding energy on top of the apex atoms; the binding site is the hollow site at the centre of the triangle between the apex and second-layer atoms. As seen in figure 2(c), the position of Xe in the gap between the tip and surface is not favoured for small tip-sample separation. Accordingly, Xe prefers to stay behind or in front of the tip where the attractive interaction energy is increased.

In figure 3, we show the variation of the minimum potential energy  $U$  and height  $\zeta$  of Xe for different positions of the tip located  $5.0$  Å above the Ni(110) surface and on the [100] line bisecting the unit cell. In fact, figure 3 presents the cross-sections of the potential energy surfaces in figure 2(c) corresponding to the tip located at different positions (shown by triangles) along the [100] direction on the Ni(110) unit cell. The minima of the potential energy curves are the possible positions of the Xe atom as it is pulled or pushed by the W(111) tip. The role of the tip in the controlled translation is clearly demonstrated in these curves. The proximity of the tip creates various minima in the potential energy; these minima follow the moving tip. Depending on the position of Xe trapped in one of these minima (i.e. in front of or behind the apex of the tip but closer to the substrate surface) different modes of controlled motion (i.e. pushing or pulling modes, respectively) are defined. Moreover, for some specific tip-sample distances, there is a local minimum in

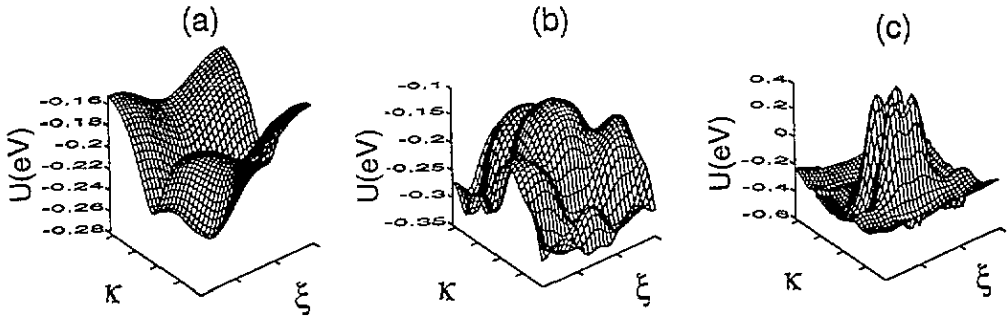


Figure 2. (a) The potential energy surface of Xe on the Ni(110) surface. (b) The same for Xe on the W(111) tip. (c) The total potential energy of Xe on the Ni(110) surface together with a W(111) tip lying 5.0 Å above the surface. The last surface plot covers a  $(3 \times 3)$  cell of the Ni(110) surface.

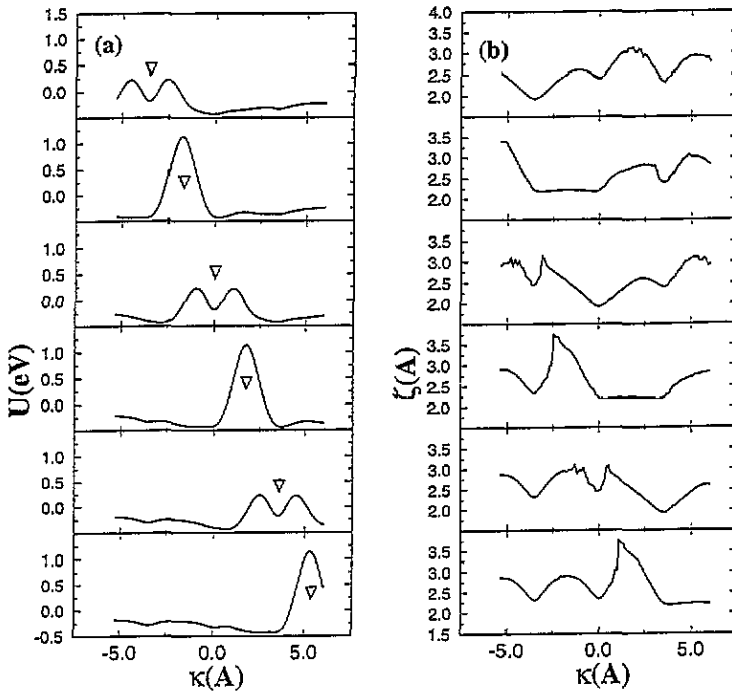
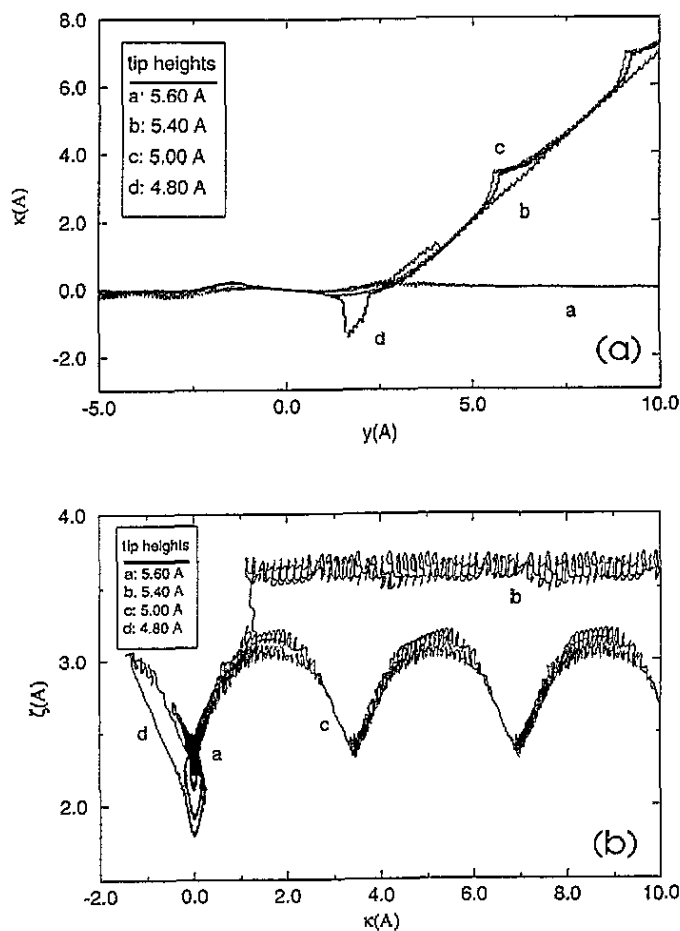


Figure 3. Variation of minimum energy  $U$  and corresponding height  $\zeta$  of Xe for a given position of the tip on the Ni(110) surface. The tip lies 5.0 Å above the Ni(110) atomic plane at a point on the [100] line bisecting the unit cell. The position of the tip in each panel is marked by a triangle. (Direction of motion can be deduced from figure 1.)

the  $U(\kappa)$  curve for which Xe becomes either closer or attached to the surface of the W tip. The sudden rise of  $\zeta$  in figure 3 corresponds to this case. Various modes in the controlled motion of Xe will be examined in detail in the next section.



**Figure 4.** (a) Lateral translation of the Xe atom induced by the tip moving along the [100] direction with preset height above the Ni(110) surface.  $y$  and  $\kappa$  are the coordinates of the tip and Xe atom along the [100] direction, respectively. (b) The variation of height  $\zeta$  of the Xe atom during the lateral translation.

#### 4. Controlled lateral translation: dynamics

The carriage of Xe on the rigid Ni(110) surface as a function of the height of the rigid tip is studied by performing molecular dynamics calculations. Figure 4(a) presents the results for the motion along the [100] direction (or  $y$  direction) where the tip starts to move towards the Xe atom from a distance. For the height of the tip  $z \geq 5.6 \text{ \AA}$  the adsorbed Xe is not practically affected by the moving tip (curve a). On the other hand, the Xe atom is attached to the moving tip for the height of the tip  $z = 5.4 \text{ \AA}$  (curve b). This is the contamination of the tip by Xe. For  $z \leq 5 \text{ \AA}$ , Xe moves behind the tip and experiences periodic jumps across the short bridge (curve c). This corresponds to the pulling mode of the lateral translation. It is interesting to note that for  $z = 4.8 \text{ \AA}$ , the Xe atom first jumps backwards for  $y - \kappa \approx 1.7 \text{ \AA}$ , and then follows the tip. The contamination and pulling mode of lateral translation are clearly shown by the variation of the height of Xe,  $\zeta$ , with its coordinate  $\kappa$ , the  $\zeta(\kappa)$  curve in figure 4(b). Note that in curve b the height of Xe,  $\zeta$ ,

is unaltered. In figure 5, we show the variation of  $\kappa$ , height  $\zeta$ , lateral and perpendicular components of the force on the Xe atom exerted by the Ni surface and W tip.

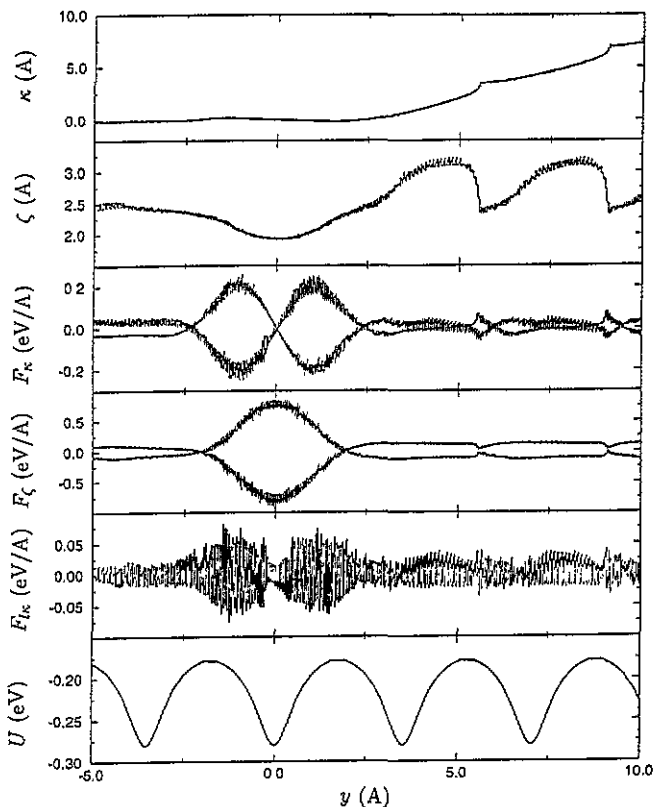


**Figure 5.** Variation of lateral coordinate  $\kappa$  and height  $\zeta$  of Xe; components of forces on the Xe atom exerted by the Ni(110) surface and the tip; variation of potential with the  $y$  coordinate of the tip moving at constant height,  $z = 5.0$  Å.

Two different modes of lateral translation of Xe, i.e. pulling and pushing modes can be distinguished in the motion of the tip along the  $[1\bar{1}0]$  direction (or  $x$  direction). While for  $\zeta \geq 5.4$  Å the Xe atom is pulled by the tip (curve b in figure 6(a)), it is pushed for  $\zeta \leq 5.3$  Å (curve c in figure 6(a)). If the tip moves along the body diagonal of the surface unit cell (or  $[112]$  direction) the Xe atom performs zig-zag motion as seen in figure 6(b). For the tip height  $z \simeq 5.5$  Å the Xe atom follows the tip by jumping to the adjacent H site. The jump along the  $[100]$  direction is followed by a jump along the  $[1\bar{1}0]$  direction, thus the zig-zags of the  $\kappa(\zeta)$  curve are quite sharp (curve a). However, for relatively smaller height ( $z \simeq 5$  Å) the zig-zags are not sharp owing to the increased tip-atom interaction. In this case, the Xe atom follows the tip between two adjacent H sites along the body diagonal without performing a vertical jump (curve b).

The relaxation of electrodes becomes important when the height of the tip  $z$  is smaller than the sum of their atomic radii. Owing to the close proximity of the tip one expects that the structure of the apex of the tip and also the values of  $Q_L$  and  $Q_S$  are modified. The relaxation is considered by including all the terms in equation (2) and by allowing all the atoms (Xe, as well as tip and sample atoms at the close proximity of the tip) to move under the force exerted by the rest of the system. The parameters of the empirical



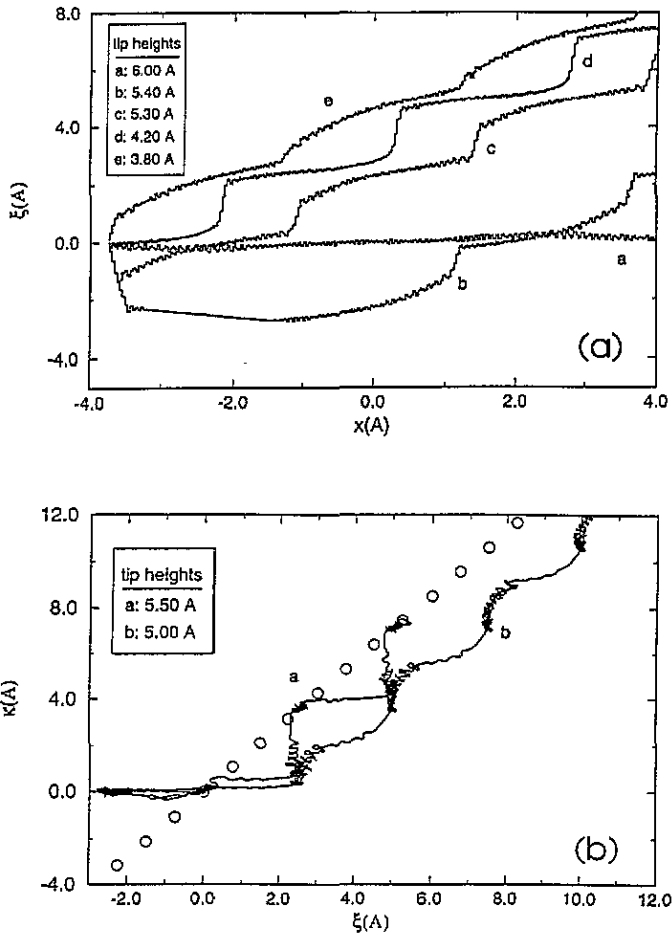


Figure 6. (a) Lateral translation of Xe controlled by the tip moving along the  $[1\bar{1}0]$  direction (specified as the  $x$  direction). (b) Trajectory of the Xe atom following the tip moving along the body diagonal of the Ni(110) unit cell (or  $[112]$  direction).  $(\kappa, \xi)$  and  $(x, y)$  are the coordinates of the Xe and tip, respectively.

potential for t-t and s-s interactions are obtained from the experimental data, whereas the parameters related to t-s interaction are determined by averaging those of bulk Ni and W. In the calculations with relaxed electrodes we used a relatively small number of atoms treated within the periodic boundary conditions. In this case, the substrate has 10 Ni(110) layers each having 375 Ni atoms, and the tip is constructed from 14 layers having a total of 560 W atoms.

Upon relaxation the tip and substrate atoms start to move around their equilibrium positions. This gives rise to fluctuations in the value of force acting on the Xe atom. For the same reasons energy can be transferred from the tip (moving agent) and also from Xe to the substrate by way of friction. Eventually, part of this energy returns to the Xe, but the remaining part raises the temperature of the system if the whole system is finite and isolated from the environment. The energy transfer becomes crucial if the speed of the tip is high. In this case the Xe atom can jump more than one unit cell even sideways. This is exactly what we obtained for high tip speeds. Another effect of the relaxation is the symmetry

breaking along  $[100]$  and  $[1\bar{1}0]$  directions. As a result, in certain conditions the Xe atom starts to escape sideways. Important effects of the electrode relaxation are summarized in figure 7. The tip is displaced in steps of  $0.88 \text{ \AA}$ . The initial condition of each tip step is taken as the configuration of the previous step. While the Xe atom is only pulled by the rigid tip at  $z = 5.0 \text{ \AA}$ , the motion proceeds in the pushing mode in the case of relaxed electrodes.

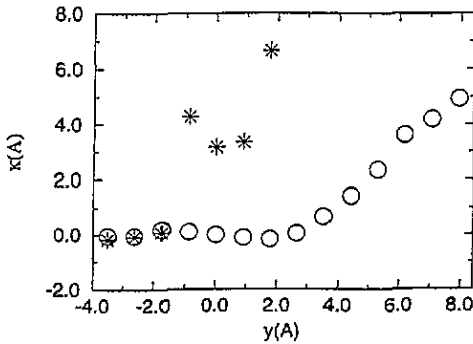


Figure 7. Displacement  $\kappa$  of Xe versus displacement  $y$  of the tip along the  $[100]$  direction bisecting the surface unit cell. Circle and stars corresponds to the rigid and relaxed electrodes, respectively. The tip height is constant,  $z = 5.0 \text{ \AA}$ .

## 5. Discussion and conclusion

Controlled motion of adatoms and their relocation at desired sites is a novel result and may lead to a wide range of applications ranging from nanoscale modifications of matter to exotic atom writing. The tip-induced modification of giant molecules and surfaces may lead to unusual properties of matter. By ordering adatoms one can obtain new superstructures on the surfaces and new electronic structures. The practical applications of controlled motion and relocation resulting in nanoscale modifications are expected to involve strongly bound adatoms. The controlled motion and relocation of noble gas adatoms may not lead to important applications, but it provides a prototype system to perform calculations to reveal crucial aspects.

The interactions between a noble gas atom and metal surface can be expressed by empirical two-body potentials. Three-body and chemical interaction can be better described by additional terms in the empirical potential. We nevertheless used a two-body potential since the available experimental data is limited and does not allow us to employ additional parameters. For the some reason we do not attempt to obtain an accurate simulation of the Eigler–Schweizer experiment, but we try to reveal some important aspects of controlled motion of weakly bound adatoms. The controlled motion of strongly bound atoms requires fully relaxed treatment by using a different kind of method for the potential (embedded atom method or self-consistent field LDA calculations).

The present calculations using empirical two-body potentials indicate that the Xe atom is bound at the H site, and the energy barrier between two adjacent H sites is lower across the long bridge than across the short bridge. The proximity of the tip lowers the potential and hence attracts the Xe atom. In this respect, a tip material having binding energy stronger than that of the sample surface is crucial for the controlled motion of the atom.

Three different types of motion of the atom are distinguished depending on the height of the tip and its direction of motion. The transfer of Xe from the sample surface to the tip may occur if the tip atoms have stronger attraction. However, owing to the pyramidal shape of the tip the attraction is weakened and the tip is prevented from permanent contamination. On the other hand a blunt tip is contaminated easily by Xe. In this case the transfer of Xe back to the sample surface does not occur. As a result the tip carrying the atom or contamination occurs only in a certain range of tip–surface distance, where Xe experiences stronger attraction from the tip than from the sample surface. For the tip material providing weaker binding than the sample surface the carriage of the adatom by the tip may not occur. The pushing mode, where the tip pushes the adatom in the direction of motion, occurs at small  $z$  and for a certain orientation of the tip and also for a certain direction of motion. The motion in the pushing mode is less stable than the pulling mode. In the pulling mode the adatom follows the tip moving at intermediate height ( $5.6 \text{ \AA} \leq z \leq 5.0 \text{ \AA}$ ). This is the sliding of the adatom in the minimum of potential energy occurring behind the tip. Self-consistent field pseudopotential calculations showed that the potential energy minima of a similar kind can be created by the tip also for chemisorbed species [8]. In this case the distance of the tip to the adatom is relatively small and requires better control of the tip. Moreover, the stability of the apex, as well as the atom transfer between tip and sample became important. The elastic modification of the atomic structure at close proximity is expected to be crucial at small tip–sample distance. Therefore, the controlled motion of a strongly bound (open-shell) atom requires fully relaxed calculations.

## Acknowledgments

This project is partially supported by the TUBITAK grant TBAG-1085.

## References

- [1] Eigler D M and Schweizer E K 1990 *Nature* **344** 524
- [2] Persson B N J and Baraloff A 1987 *Phys. Rev. Lett.* **59** 339  
Lyo I W and Avouris P 1991 *Science* **253** 173
- [3] Eigler D M, Lutz C P and Rudge W E 1991 *Nature* **352** 600
- [4] For a comprehensive discussion of short- and long-range interaction see for example Ciraci S et al 1992 *Phys. Rev. B* **46** 10411. For the application of tip–sample interactions see Ciraci S 1990 *Basic Concepts and Applications of Scanning Tunneling Microscopy and Related Techniques* ed H Rohrer, N Garcia and J Behm (Dordrecht: Kluwer) section 119
- [5] Lifshitz E M 1956 *Sov. Phys.-JETP* **2** 73
- [6] Israelachvili J N 1985 *Intermolecular and Surface Forces* (London: Academic)
- [7] Ciraci S and Baratoff A unpublished  
Ciraci S 1992 *Atomic and Nanometer-scale Modifications of Materials: Fundamentals and Applications* (Dordrecht: Kluwer) section 111
- [8] Perez R, Garcia-Videl F C, de Andres P L and Flores F 1994 *Surf. Sci.* **307** 704
- [9] Scheider U, Castro G R, Isern H, Janssens T and Wandelt K 1991 *Surf. Sci.* **251/252** 551
- [10] Buldum A and Ciraci S unpublished  
Müller J E 1990 *Phys. Rev. Lett.* **65** 3021  
Eigler D M, Weiss P S, Schweizer E K and Lang N D 1991 *Phys. Rev. Lett.* **66** 1189
- [11] Morse M D 1986 *Chem. Rev.* **86** 1043
- [12] Huber K P and Herzberg G 1979 *Constants of Diatomic Molecules* (New York: Van Nostrand Reinhold)
- [13] Nieuwenhuys B E, Van Aardenne O G and Sachter W M H 1974 *Chem. Phys.* **5** 418
- [14] Dresser M J, Madey T E and Yates J T 1974 *Surf. Sci.* **42** 533
- [15] Cerda J R, de Andres P L, Flores F and Perez R 1992 *Phys. Rev. B* **45** 8721